Nuclear matrix elements for Majoron-emitting double-β decay

J. Kotila [1,2,*] and F. Iachello [2,†]

[1] *Finnish Institute for Educational Research, University of Jyväskylä, P.O. Box 35, 40014 Jyväskylä, Finland*

[2] *Center for Theoretical Physics, Sloane Physics Laboratory Yale University, New Haven, Connecticut 06520-8120, USA*

(Received 3 November 2020; accepted 18 March 2021; published 1 April 2021)

A complete calculation of the nuclear matrix elements (NMEs) for Majoron emitting neutrinoless double beta decay within the framework of IBM-2 for spectral indices $n = 1, 3, 7$ is presented. By combining the results of this calculation with previously calculated phase-space factors (PSFs) we give predictions for expected half-lives. By comparing with experimental limits on the half-lives we set limits on the coupling constants $\langle g_{ee}^M \rangle$ of all proposed Majoron-emitting models.

DOI: 10.1103/PhysRevC.103.044302

I. INTRODUCTION

In recent years, increased accuracy has been achieved in the measurement of double-β decay (DBD) with the emission of two neutrinos, $2\nu\beta\beta$ decay, especially in the measurement of the summed electron spectra. High-statistics experiments have been reported by GERDA (^{76}Ge) [1], NEMO3 (^{100}Mo) [2], CUORE (^{130}Te) [3], EXO (^{136}Xe) [4], and KamLAND-Zen (^{136}Xe) [5]. High-statistics experiments have provided information on the mechanism of DBD in $2\nu\beta\beta$ decay, in particular on the question of single-state dominance (SSD) versus high-state dominance (HSD), CUPID-0 (^{82}Se) [6] and CUPID-Mo (^{100}Mo) [7]. With the degree of accuracy reached in the latest experiments, one can also test nonstandard mechanisms of DBD and set stringent limits on them [8].

One of the nonstandard mechanisms is that occurring with the emission of additional bosons called Majorons. Majorons were introduced years ago [10,11] as massless Nambu-Goldstone bosons arising from global $B - L$ (baryon number minus lepton number symmetry) broken spontaneously in the low-energy regime. These bosons couple to the Majorana neutrinos and give rise to neutrinoless double-β decay, accompanied by Majoron emission $0\nu\beta\beta M$ [12], as schematically shown in Fig. 1(a). Although these older models are disfavored by precise measurements of the width of the Z boson decay to invisible channels [13], several other models of $0\nu\beta\beta M$ decay have been proposed in which one or two Majorons, denoted by χ_0, are emitted (see Fig. 1):

$$\begin{aligned}(A, Z) &\rightarrow (A, Z+2) + 2e^- + \chi_0,\\ (A, Z) &\rightarrow (A, Z+2) + 2e^- + 2\chi_0.\end{aligned} \tag{1}$$

Table I lists some of the models proposed to describe these decays [14–17]. The different models are distinguished by the nature of the emitted Majoron(s), i.e., whether it is a Nambu-Goldstone boson (NG), the leptonic charge of the emitted Majoron (L), and the spectral index of the model, n.

The half-life for all these models can be written as

$$\left[\tau_{1/2}^{0\nu M}\right]^{-1} = G_{m\chi_0 n}^{(0)} \left|\langle g_{\chi_{ee}^M} \rangle\right|^{2m} \left|M_{0\nu M}^{(m,n)}\right|^2, \tag{2}$$

where $G_{m\chi_0 n}^{(0)}$ is a phase-space factor (PSF), $\langle g_{\chi_{ee}^M} \rangle$ is the effective coupling constant of the Majoron to the neutrino, $m = 1, 2$ for the emission of one or two Majorons, respectively, and $M_{0\nu M}^{(m,n)}$ the nuclear matrix element (NME).

II. PHASE-SPACE FACTORS

In a previous article [9] we calculated the PSF and from these the single-electron spectrum, the summed electron spectrum, and the angular correlation between the two electrons. Particularly interesting are the summed electron spectra whose shape depends crucially on the spectral index n. In Fig. 2, the summed electron spectra for $n = 1$, $n = 3$ and $n = 7$, obtained from Ref. [9] by normalizing the spectra so that the area covered by each of them is the same, are plotted as a function of $\varepsilon_1 + \varepsilon_2 - 2m_e c^2$. In this figure, also the summed electron spectrum for $2\nu\beta\beta$ decay [18] is shown again with area normalized to 1. This spectrum has a spectral index $n = 5$. The summed electron spectrum of the "bulk" model $n = 2$ is also shown in Fig. 2. Exact Dirac wave functions, nuclear finite size, and electron screening are included in this calculation, as discussed in Ref. [18]. Previous calculations [19–22] make use of Fermi functions, which are an approximation to the relativistic Dirac wave functions. For comparison between the values reported in Ref. [22] and our values [9] we note that our PSFs are divided by a factor of $g_A^4 = 2.593$ since we include this factor in the NME. We estimated the error in using the old calculation of the PSFs [19–22] instead of the new [9], $(G_{m\chi_0 n}^{(0)old} - G_{m\chi_0 n}^{(0)new})/G_{m\chi_0 n}^{(0)new}$, to be 6% in ^{76}Ge and 28% in ^{136}Xe. The reason why the error is larger in ^{136}Xe ($Z = 54$) than in ^{76}Ge ($Z = 32$) is the neglect in the old calculation of relativistic effects and electron screening which increase as a large power of Z. While in ^{76}Ge and ^{82}Se the use of the old

*jenni.kotila@jyu.fi

†francesco.iachello@yale.edu

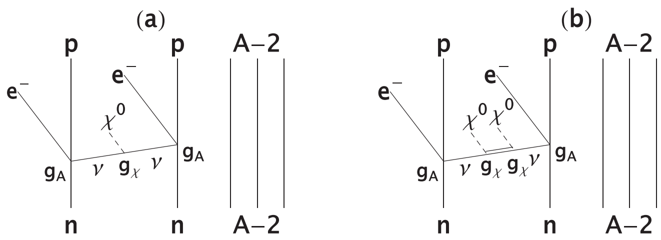

FIG. 1. Schematic representation of neutrinoless double-β decay accompanied by the emission of one or two Majorons. Adapted from Ref. [9].

calculation may still be reasonable, it is definitely not so in the other nuclei of current interest: ^{100}Mo, ^{130}Te, ^{136}Xe, and ^{150}Nd. Although experimentally not easily accessible, we also plot in Fig. 3 the single electron spectra with area normalized to 1, and in Fig. 4 the angular correlation between the two electrons, for $n = 1$, $n = 2$, $n = 3$, $n = 7$, and $2\nu\beta\beta$ ($n = 5$) as a function of $\varepsilon_1 - m_e c^2$, both of which have been measured by the NEMO3 collaboration in ^{130}Te [23]. In this article we present a calculation of the nuclear matrix elements $M_{0\nu M}^{(m,n)}$.

III. NUCLEAR MATRIX ELEMENTS

Nuclear matrix elements for Majoron-emitting DBD were derived in a seminal paper by Hirsch *et al.* [22]. These authors derived an explicit form for the nuclear matrix elements of all the models of Table I, except for the “bulk” model. We have converted the form of Ref. [22] to our notation, added some higher-order terms not included in the original form and calculated the corresponding matrix elements within the framework of the microscopic interacting boson model IBM-2 [24,25] with isospin restoration [26]. Explicitly, we introduce the matrix elements

$$\begin{aligned}\mathcal{M}_F &= \langle f\|v_m\|i\rangle,\\ \mathcal{M}_{GT} &= \langle f\|v_m\boldsymbol{\sigma}_1\cdot\boldsymbol{\sigma}_2\|i\rangle,\\ \mathcal{M}_T &= \langle f\|v_m S_{12}\|i\rangle,\end{aligned}$$

TABLE I. Different Majoron-emitting models [14–17]. The third, fourth, and fifth columns indicate whether the Majoron is a Nambu-Goldstone boson, its leptonic charge L, and the model's spectral index, n. The sixth column indicates the nuclear matrix elements of Sec. II appropriate for each model.

Model	Decay mode	NG boson	L	n	NME
IB	$0\nu\beta\beta\chi_0$	No	0	1	M_1
IC	$0\nu\beta\beta\chi_0$	Yes	0	1	M_1
ID	$0\nu\beta\beta\chi_0\chi_0$	No	0	3	M_3
IE	$0\nu\beta\beta\chi_0\chi_0$	Yes	0	3	M_3
IIB	$0\nu\beta\beta\chi_0$	No	−2	1	M_1
IIC	$0\nu\beta\beta\chi_0$	Yes	−2	3	M_2
IID	$0\nu\beta\beta\chi_0\chi_0$	No	−1	3	M_3
IIE	$0\nu\beta\beta\chi_0\chi_0$	Yes	−1	7	M_3
IIF	$0\nu\beta\beta\chi_0$	Gauge boson	−2	3	M_2
“Bulk”	$0\nu\beta\beta\chi_0$	Bulk field	0	2	

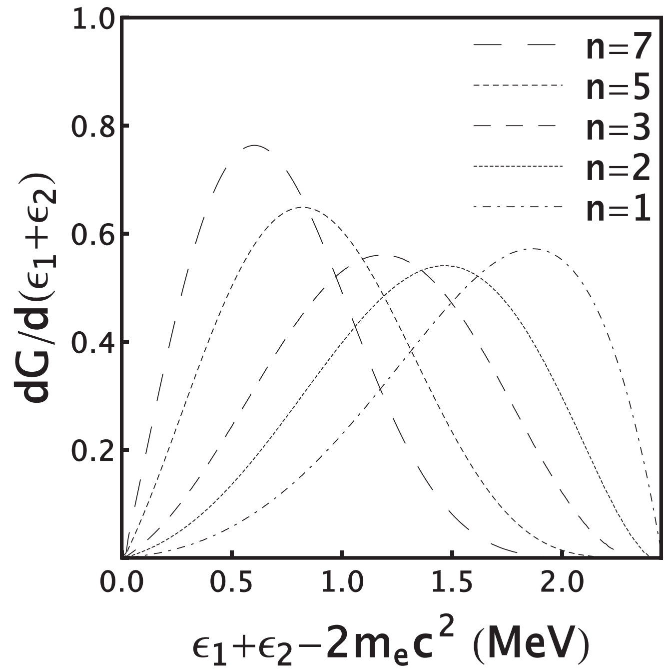

FIG. 2. Summed electron spectra for the $n = 1$, 2, 3, and 7, as well as for the $2\nu\beta\beta$ ($n = 5$) decays of ^{136}Xe.

$$\begin{aligned}\mathcal{M}_{GTR} &= \langle f\|v_R\boldsymbol{\sigma}_1\cdot\boldsymbol{\sigma}_2\|i\rangle,\\ \mathcal{M}_{TR} &= \langle f\|v_R S_{12}\|i\rangle,\\ \mathcal{M}_{F\omega^2} &= \langle f\|v_{\omega^2}\|i\rangle,\\ \mathcal{M}_{GT\omega^2} &= \langle f\|v_{\omega^2}\boldsymbol{\sigma}_1\cdot\boldsymbol{\sigma}_2\|i\rangle,\\ \mathcal{M}_{T\omega^2} &= \langle f\|v_{\omega^2}S_{12}\|i\rangle,\end{aligned} \tag{3}$$

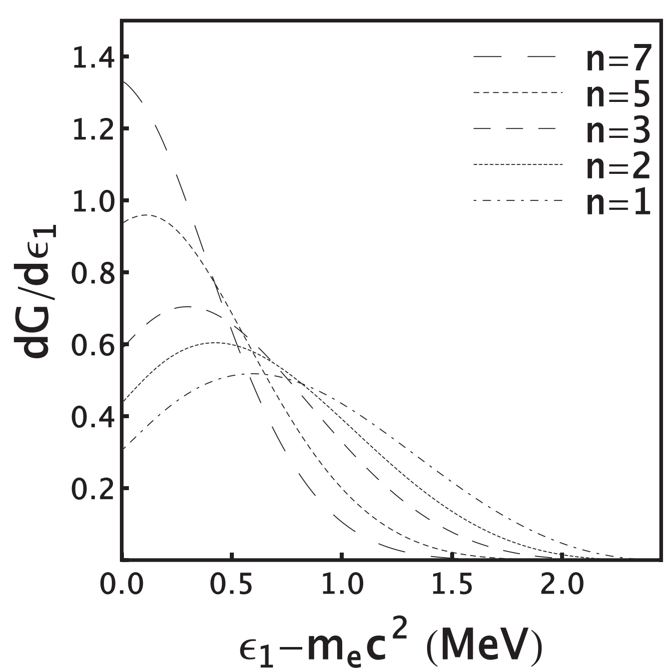

FIG. 3. Single electron spectra for the $n = 1$, 2, 3, and 7, as well as for the $2\nu\beta\beta$ ($n = 5$) decays of ^{136}Xe.

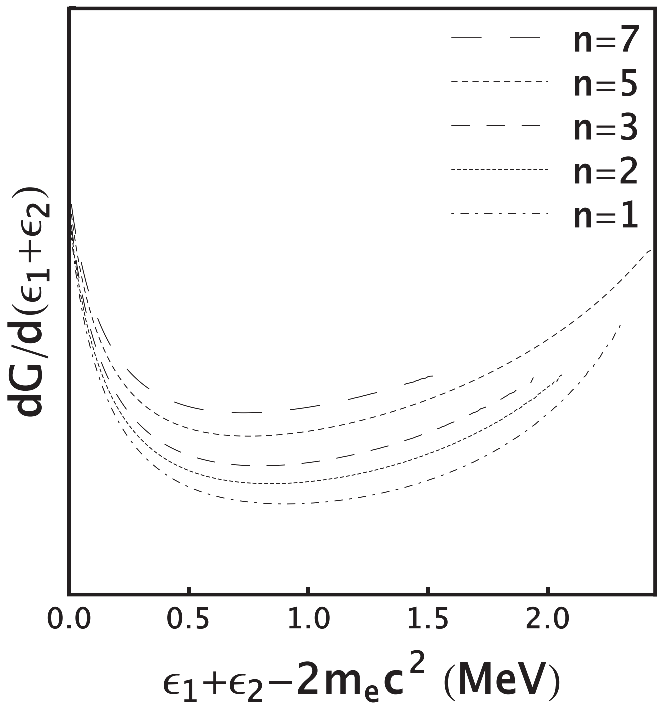

FIG. 4. Angular correlation between the two emitted electrons for the $n = 1, 2, 3$, and 7, as well as for the $2\nu\beta\beta$ ($n = 5$) decays of ^{136}Xe. The calculation for $n = 1, 2, 3, 7$ stops at the point where the single electron spectrum goes to zero. Beyond that point it becomes unstable as $G^{(0)}$ goes to zero faster than $G^{(1)}$. For $2\nu\beta\beta$ ($n = 5$) this is avoided by taking into account the individual energies of the neutrinos, ω_1 and ω_2, as in Eq. (22) of Ref. [18], instead of the Majoron energy q as in Eq. (5) of Ref. [9].

where the isospin operators $\tau_1^+\tau_2^+$ have been dropped for simplicity. These matrix elements are the same as in Ref. [22] with the addition of the tensor matrix elements.

The neutrino potentials needed for the calculation of these matrix elements, when converted to the notation used in IBM-2 [24–26] are

$$v_m = \frac{2}{\pi}\frac{1}{q(q+\tilde{A})}, \quad v_R = \frac{2}{\pi}\frac{1}{Rm_p}\frac{q+\frac{\tilde{A}}{2}}{q(q+\tilde{A})^2},$$
$$v_{\omega^2} = \frac{2}{\pi}m_e^2\frac{q^2+\frac{9}{8}q\tilde{A}+\frac{3}{8}\tilde{A}^2}{q^3(q+\tilde{A})^3}, \tag{4}$$

with $R = 1.2A^{1/3}$ fm, $m_p = 938$ MeV $= 4.76$ fm^{-1}, $m_e = 0.511$ MeV $= 0.00259$ fm^{-1}. $\tilde{A}$ is the closure energy that we take as in Refs. [24–26], $\tilde{A} = 1.12A^{1/2}$ MeV, where A denotes the mass number. We note that the last term in v_{ω^2} diverges at the origin as q^{-3}. We regularize this term by multiplying it by $q/(q+\tilde{A})$, that is

$$v_{\omega^2} = \frac{2}{\pi}m_e^2\frac{q^2+\frac{9}{8}q\tilde{A}+\frac{3}{8}\tilde{A}^2\frac{q}{q+\tilde{A}}}{q^3(q+\tilde{A})^3}. \tag{5}$$

From the neutrino potentials we construct the quantities

$$h(q) = v(q)\tilde{h}(q), \tag{6}$$

where $\tilde{h}_{F,GT,T}(q) = \tilde{h}_{F\omega^2,GT\omega^2,T\omega^2}$ are given in Table II of Ref. [25] which includes the form factors and higher-order corrections and

$$\tilde{h}_R(q) = \frac{1}{(1+q^2/m_V^2)^2}\frac{1}{(1+q^2/m_A^2)^2}, \tag{7}$$

which includes the form factors with $m_V = 0.84$ GeV and $m_A = 1.09$ GeV, as in Refs. [25,26].

The matrix elements for the three classes of Majoron models are

$$M_1 = g_A^2\mathcal{M}_1 = g_A^2\left[-\left(\frac{g_V^2}{g_A^2}\right)\mathcal{M}_F + \mathcal{M}_{GT} - \mathcal{M}_T\right],$$
$$M_2 = g_A^2\mathcal{M}_2 = g_A^2\left[\left(\frac{g_V}{g_A}\right)\frac{f_W}{3}\mathcal{M}_{GTR} - \left(\frac{g_V}{g_A}\right)\frac{f_W}{6}\mathcal{M}_{TR}\right],$$
$$M_3 = g_A^2\mathcal{M}_3 = g_A^2\left[-\left(\frac{g_V^2}{g_A^2}\right)\mathcal{M}_{F\omega^2} + \mathcal{M}_{GT\omega^2} - \mathcal{M}_{T\omega^2}\right], \tag{8}$$

where we have used the overall sign convention as in Ref. [27] and in our previous papers [24–26]. In Eq. (8), $f_W = 1 + \kappa_\beta = 4.70$, where κ_β is the isovector magnetic moment of the nucleon. In the calculation of the matrix elements in Eq. (8) also short-range correlations are included as in Refs. [24–26]. Our results are shown in Table II. The nuclear matrix elements M_1, M_2, M_3 are associated with Majoron-emitting models of $0\nu\beta\beta M$ decays as in the last column of Table I.

Sensitivity to parameter changes, model assumptions, and operator assumptions

The matrix element $\mathcal{M}_1$ for index $n = 1$ is identical to the matrix element of ordinary $0\nu\beta\beta$ decay without Majoron emission. The sensitivity of IBM-2 calculations to parameter changes, model assumptions, and operator assumption for this NME was discussed in great detail in Refs. [25,26]. Our error estimate for M_1 is therefore 16% for all nuclei, as in Ref. [26].

For the matrix element $\mathcal{M}_2$ we have an additional error coming from the neglect of higher-order terms of the type

$$\frac{(\mathbf{Q}\cdot\boldsymbol{\sigma}_1)(\mathbf{q}\cdot\boldsymbol{\sigma}_2)}{4m_p^2} \simeq \frac{(\mathbf{q}\cdot\boldsymbol{\sigma}_1)(\mathbf{q}\cdot\boldsymbol{\sigma}_2)}{4m_p^2}$$
$$= \frac{q^2}{4m_p^2}\left[\frac{1}{3}\boldsymbol{\sigma}_1\cdot\boldsymbol{\sigma}_2 + \frac{1}{3}S_{12}\right], \tag{9}$$

where $\mathbf{Q}$ is the total momentum and $\mathbf{q}$ the relative momentum of the nucleons and we have assumed $\mathbf{Q} \simeq \mathbf{q}$ [20]. We estimate the neglected contribution of these higher-order terms to be about 4%, giving a total estimated error of 20% for $\mathcal{M}_2$.

The matrix element $\mathcal{M}_3$ depends strongly on the closure energy $\tilde{A}$ as given in Eq. (4). In the present calculation we have assumed the standard choice $\tilde{A} = 1.12A^{1/2}$ MeV. We have investigated variations of $\tilde{A}$ around the standard values and estimate an additional error in the calculation of $\mathcal{M}_3$ of ≈10%, bringing the total estimated error to 30%. An estimate of the sensitivity of $\mathcal{M}_3$ to the closure energy was also given in Ref. [22]. In this reference also a discussion of the sensitivity to model assumptions of Majoron-emitting DBD was given.

TABLE II. Majoron-emitting DBD NMEs $\mathcal{M}_i$ ($i = 1, 2, 3$) calculated in this work using the quenched value $g_A = 1.0$ and the convention $\mathcal{M}_i > 0$.

Isotope	$\mathcal{M}_F$	$\mathcal{M}_{GT}$	$\mathcal{M}_T$	$\mathcal{M}_1$	$\mathcal{M}_{GTR}$	$\mathcal{M}_{TR}$	$\mathcal{M}_2$	$\mathcal{M}_{F\omega^2}$ $\times 10^3$	$\mathcal{M}_{GT\omega^2}$ $\times 10^3$	$\mathcal{M}_{T\omega^2}$ $\times 10^3$	$\mathcal{M}_3$ $\times 10^3$
^{76}Ge	−0.780	5.582	−0.281	6.642	0.225	−0.037	0.381	−0.017	2.530	−0.009	2.556
^{82}Se	−0.667	4.521	−0.270	5.458	0.178	−0.034	0.305	−0.014	1.967	−0.009	1.993
^{96}Zr	−0.361	3.954	0.250	4.065	0.147	0.031	0.205	−0.006	1.672	0.009	1.668
^{100}Mo	−0.511	5.075	0.318	5.268	0.187	0.038	0.263	−0.008	1.904	0.011	1.901
^{110}Pd	−0.425	4.024	0.243	4.206	0.144	0.030	0.203	−0.006	1.411	0.009	1.409
^{116}Cd	−0.335	2.888	0.118	3.105	0.102	0.019	0.144	−0.005	0.945	0.006	0.945
^{124}Sn	−0.572	3.099	−0.118	3.789	0.104	−0.017	0.177	−0.013	1.161	−0.005	1.179
^{128}Te	−0.718	3.965	−0.115	4.798	0.132	−0.020	0.223	−0.016	1.505	−0.006	1.527
^{130}Te	−0.651	3.586	−0.159	4.396	0.118	−0.018	0.199	−0.014	1.291	−0.005	1.311
^{134}Xe	−0.686	3.862	−0.121	4.669	0.126	−0.018	0.212	−0.015	1.456	−0.006	1.477
^{136}Xe	−0.522	2.958	−0.123	3.603	0.096	−0.013	0.160	−0.012	1.161	−0.004	1.112
^{148}Nd	−0.362	2.283	0.125	2.521	0.074	0.012	0.107	−0.006	0.648	0.004	0.650
^{150}Nd	−0.507	3.371	0.119	3.759	0.110	0.017	0.159	−0.008	0.836	0.005	0.839
^{154}Sm	−0.340	2.710	0.122	2.928	0.086	0.015	0.122	−0.006	0.858	0.005	0.859
^{160}Gd	−0.415	3.838	0.250	4.002	0.120	0.023	0.170	−0.006	1.261	0.008	1.260
^{198}Pt	−0.329	2.021	0.119	2.230	0.061	0.009	0.089	−0.005	0.393	0.003	0.395
^{232}Th	−0.444	3.757	0.251	3.950	0.104	0.019	0.148	−0.006	0.930	0.007	0.930
^{238}U	−0.525	4.470	0.244	4.751	0.122	0.022	0.174	−0.007	1.118	0.008	1.118

IV. LIMITS ON THE COUPLING CONSTANTS

From the PSF of Ref. [9], the NME of this article, and experimental limits on half-lives for each type of Majoron model, one can derive limits on the coupling constants $g_{\chi^M_{ee}}$. These limits depend on the value of the coupling constant g_A. This coupling constant is renormalized in nuclei by many-body effects. Three possible values are [28] (i) the free

TABLE III. Limits on the Majoron-neutrino coupling constants $\langle g_{\chi^M_{ee}} \rangle$ for $g_A = 1$. PSF from Ref. [9]. NME from this paper.

Decay mode	Spectral index	Model type	$\mathcal{M}$	$G^{(0)}_{m\chi_0 n}[10^{-18}$ yr]	$\tau_{1/2}$ [yr]	$\lvert\langle g_{\chi^M_{ee}}\rangle\rvert$
^{76}Ge [32]						
$0\nu\beta\beta\chi_0$	1	IB,IC,IIB	6.64	44.2	$>4.2 \times 10^{23}$	$<3.5 \times 10^{-5}$
$0\nu\beta\beta\chi_0\chi_0$	3	ID,IE,IID	0.0026	0.22	$>0.8 \times 10^{23}$	<1.7
$0\nu\beta\beta\chi_0$	3	IIC,IIF	0.381	0.073	$>0.8 \times 10^{23}$	$<0.34 \times 10^{-1}$
$0\nu\beta\beta\chi_0\chi_0$	7	IIE	0.0026	0.420	$>0.3 \times 10^{23}$	<1.9
$0\nu\beta\beta\chi_0$	2	Bulk			$>1.8 \times 10^{23}$	
^{130}Te [29]						
$0\nu\beta\beta\chi_0$	1	IB,IC,IIB	4.40	413	$>2.2 \times 10^{21}$	$<2.4 \times 10^{-4}$
$0\nu\beta\beta\chi_0\chi_0$	3	ID,IE,IID	0.0013	3.21	$>0.9 \times 10^{21}$	<3.8
$0\nu\beta\beta\chi_0$	3	IIC,IIF	0.199	1.51	$>2.2 \times 10^{21}$	$<0.87 \times 10^{-1}$
$0\nu\beta\beta\chi_0\chi_0$	7	IIE	0.0013	14.4	$>0.9 \times 10^{21}$	<2.6
$0\nu\beta\beta\chi_0$	2	Bulk			$>2.2 \times 10^{21}$	
^{130}Te [23]						
$0\nu\beta\beta\chi_0$	1	IB,IC,IIB	4.40	413	$>1.6 \times 10^{22}$	$<8.8 \times 10^{-5}$
^{136}Xe [31]						
$0\nu\beta\beta\chi_0$	1	IB,IC,IIB	3.60	409	$>1.2 \times 10^{24}$	$<1.3 \times 10^{-5}$
$0\nu\beta\chi_0\chi_0$	3	ID,IE,IID	0.0011	3.05	$>2.7 \times 10^{22}$	<1.8
$0\nu\beta\beta\chi_0$	3	IIC,IIF	0.160	1.47	$>2.7 \times 10^{22}$	$<0.31 \times 10^{-1}$
$0\nu\beta\beta\chi_0\chi_0$	7	IIE	0.0011	12.5	$>6.1 \times 10^{21}$	<1.8
$0\nu\beta\beta\chi_0$	2	Bulk			$>2.5 \times 10^{23}$	
^{136}Xe [30]						
$0\nu\beta\beta\chi_0$	1	IB,IC,IIB	3.60	409	$>2.6 \times 10^{24}$	$<8.5 \times 10^{-6}$
$0\nu\beta\beta\chi_0\chi_0$	3	ID,IE,IID	0.0011	3.05	$>4.5 \times 10^{24}$	<0.49
$0\nu\beta\beta\chi_0$	3	IIC,IIF	0.160	1.47	$>4.5 \times 10^{24}$	$<0.24 \times 10^{-2}$
$0\nu\beta\beta\chi_0\chi_0$	7	IIE	0.0011	12.5	$>1.1 \times 10^{22}$	<1.6
$0\nu\beta\beta\chi_0$	2	Bulk			$>1.0 \times 10^{24}$	

value, $g_A = 1.269$, (ii) the quark value, $g_A = 1.0$, and (iii) the value extracted from $2\nu\beta\beta$ decay, which, in IBM-2 can be parametrized as $g_{A,eff}^{IBM-2} = 1.269A^{-0.18}$. To allow for different values of g_A, we rewrite Eq. (2) as

$$\left[\tau_{1/2}^{0\nu M}\right]^{-1} = G_{m\chi_0 n}^{(0)}\left|\langle g_{\chi_{ee}^M}\rangle\right|^{2m} g_A^4 \left|\mathcal{M}_{0\nu M}^{(m,n)}\right|^2, \quad (10)$$

where $\mathcal{M}_{0\nu M}^{(m,n)}$ are the NME given in Table II. In extracting limits on $g_{\chi_{ee}^M}$ we use in this article $g_A = 1$. From Eq. (10) it is straightforward to obtain limits for other values of g_A.

Limits on half-lives for Majoron-emitting models have been reported by several groups [23,29–32]. In Table III we provide our limits on the coupling constants $g_{\chi_{ee}^M}$.

The most stringent limits come from the KamLAND-Zen collaboration [30] and from the EXO collaboration [31]. The reason why one obtains such small limits for Majoron-emitting models with index $n = 1$ was discussed in Ref. [22]. The larger limits of $g_{\chi_{ee}^M}$ for Majoron-emitting models with index $n = 3$ and $n = 7$ are due to the smaller values of the PSF for these indices.

V. CONCLUSIONS

We have presented here a complete calculation of NME for Majoron-emitting neutrinoless double-β decay within the framework of the Interacting Boson Model IBM-2. Our results when combined with the phase space factors of Ref. [9] provide up-to-date predictions for lifetimes, single-electron spectra, summed electron spectra, and angular distributions for Majoron-emitting neutrinoless double-β decay which can be used in the analysis of recent high-statistics experiments [1–7].

ACKNOWLEDGMENTS

This work was supported in part by the Academy of Finland Grants No. 314733 and No. 320062.

[1] M. Agostini *et al.* (GERDA Collaboration), Nature (London) **544**, 47 (2017).
[2] R. Arnold *et al.* (NEMO3 Collaboration), Phys. Rev. D **92**, 072011 (2015).
[3] K. Alfonso *et al.* (CUORE Collaboration), Phys. Rev. Lett. **115**, 102502 (2015).
[4] N. Ackerman *et al.* (EXO Collaboration), Phys. Rev. Lett. **107**, 212501 (2011).
[5] A. Gando *et al.* (KamLAND-Zen Collaboration), Phys. Rev. C **85**, 045504 (2012).
[6] O. Azzolini *et al.* (CUPID-0 Collaboration), Phys. Rev. Lett. **123**, 262501 (2019).
[7] E. Armengaud *et al.*, Eur. Phys. J. C **80**, 674 (2020).
[8] F. F. Deppisch, L. Graf, and F. Šimkovic, Phys. Rev. Lett. **125**, 171801 (2020).
[9] J. Kotila, J. Barea, and F. Iachello, Phys. Rev. C **91**, 064310 (2015).
[10] Y. Chikashige, R. N. Mohapatra, and R. D. Peccei, Phys. Rev. Lett. **45**, 1926 (1980).
[11] G. B. Gelmini and M. Roncadelli, Phys. Lett. B **99**, 411 (1981).
[12] H. M. Georgi, S. L. Glashow, and S. Nussinov, Nucl. Phys. B **193**, 297 (1981).
[13] The ALEPH Collaboration, DELPHI Collaboration, L3 Collaboration, OPAL Collaboration, SLD Collaboration, LEP Electroweak Working Group, and Electroweak and Heavy Flavor Group, Phys. Rep. **427**, 257 (2006).
[14] P. Bamert, C. Burgess, and R. Mohapatra, Nucl. Phys. B **449**, 25 (1995).
[15] C. D. Carone, Phys. Lett. B **308**, 85 (1993).
[16] C. Burgess and J. Cline, in *Proceedings of the First International Conference on Nonaccelerator Physics, Bangalore, India, 1994*, edited by R. Cowsik (World Scientific, Singapore, 1995).
[17] R. Mohapatra, A. Perez-Lorenzana, and C. D. S. Pires, Phys. Lett. B **491**, 143 (2000).
[18] J. Kotila and F. Iachello, Phys. Rev. C **85**, 034316 (2012).
[19] M. Doi, T. Kotani, and E. Takasugi, Prog. Theor. Phys. Suppl. **83**, 1 (1985).
[20] T. Tomoda, Rep. Prog. Phys. **54**, 53 (1991).
[21] J. Suhonen and O. Civitarese, Phys. Rep. **300**, 123 (1998).
[22] M. Hirsch, H. V. Klapdor-Kleingrothaus, S. G. Kovalenko, and H. Päs, Phys. Lett. B **372**, 8 (1996).
[23] R. Arnold *et al.* (NEMO3 Collaboration), Phys. Rev. Lett. **107**, 062504 (2011).
[24] J. Barea and F. Iachello, Phys. Rev. C **79**, 044301 (2009).
[25] J. Barea, J. Kotila, and F. Iachello, Phys. Rev. C **87**, 014315 (2013).
[26] J. Barea, J. Kotila, and F. Iachello, Phys. Rev. C **91**, 034304 (2015).
[27] F. Šimkovic, G. Pantis, J. D. Vergados, and A. Faessler, Phys. Rev. C **60**, 055502 (1999).
[28] S. Dell'Oro, S. Marcocci, and F. Vissani, Phys. Rev. D **90**, 033005 (2014).
[29] C. Arnaboldi *et al.* (CUORE Collaboration), Phys. Lett. B **557**, 167 (2003).
[30] A. Gando, Y. Gando, H. Hanakago, H. Ikeda, K. Inoue, R. Kato, M. Koga, S. Matsuda, T. Mitsui, T. Nakada, K. Nakamura, A. Obata, A. Oki, Y. Ono, I. Shimizu, J. Shirai, A. Suzuki, Y. Takemoto, K. Tamae, K. Ueshima *et al.* (KamLAND-Zen Collaboration), Phys. Rev. C **86**, 021601(R) (2012).
[31] J. B. Albert *et al.* (EXO-200 Collaboration), Phys. Rev. D **90**, 092004 (2014).
[32] S. Hemmer (GERDA Collaboration), Eur. Phys. J. Plus **130**, 139 (2015).